Utrecht University

Opleiding Natuur- en Sterrenkunde

Study of charge dependent higher harmonic correlations at LHC energies

Bachelor Thesis

Tijn Visser

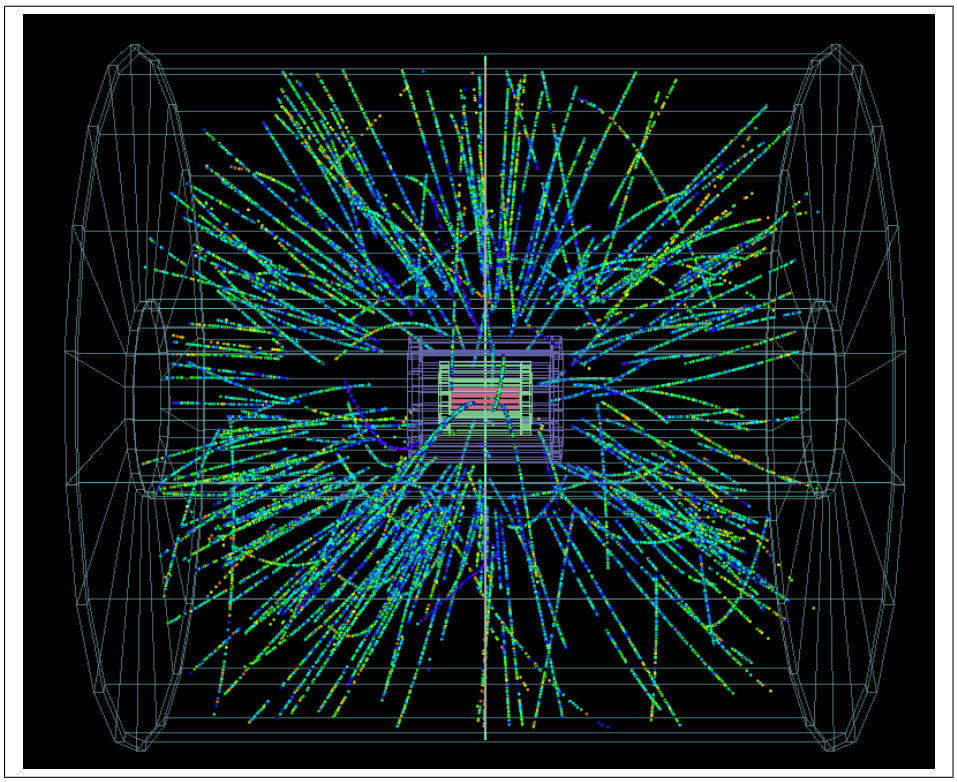

Supervisors:

Dr.Panos Christakoglou Supervisor
Nikhef / Utrecht University

June 16^{th} - 2021

Abstract

The main goal of this thesis is to understand the Chiral Magnetic Effect (CME), studied by "A Large Ion Collider Experiment" (ALICE) at the "Large Hadron Collider" (LHC). This effect is of interest, since it is found to be caused by parity-symmetry violating effects, considering the strong-nuclear force. This is a relative recent finding and could potentially have interesting implications. In order to understand this better we have used simulation data to reconstruct what takes place in the found state of matter, resulting from the collision, called Quark Gluon Plasma. For this thesis, these simulation data are used and studied by using mathematical tools, called correlators. For this thesis we have studied two of them.

The results found are however quite inconclusive. As will be described in section 5, the results suggest that more simulation data needs to be used and more configurations of input parameters need to studied, to find how these correlators can help us understand the experimental results.

The picture on the titlepage is a visualization of the products of the collision performed at ALICE. The lines in the detector display the paths the particles, comming from the collision, take. This picture is found on the CERN website (see ref. [1]).

Contents

1 Introduction

For a long time now subatomic physicists have postulated that certain symmetries are fundamental facts of the Universe. For example, take time-symmetry. When looking at the atomic scale, imagine playing a video of a simple collision between two particles (never mind that it is hard to record). Now play the video backwards. When examining these two events, one can see that both seem to satisfy our equations of motion i.e. both seem physical. This is one of the arguments to say that the Universe is time-symmetric.
One other postulate is that the strong nuclear force is parity-symmetric. Parity-symmetry could be considered the spatial sister of time-symmetry. When looking into a mirror while the same event occurs, one can observe that the laws of physics are unchanged over this transformation. Quantum Field Theory(QFT) is one of the most beloved mathematical descriptions of the Universe, which rely heavily upon these symmetries. In this thesis I will describe how, when considering the strong nuclear force, this symmetry is not fundamental. This thesis will try to help quantify the degree to which this symmetry can be broken by means of data from nuclei collisions, done at the Large Hadron Collider(LHC), together with simulation data obtained using a state-of-the-art hydro-dynamical model. Section 5 will also give advice as to how to proceed the study.
Now, how does one observe a breaking of such a symmetry? First, one needs 5 billion USD priced particle accelerator. Secondly, let some nuclei bump into each other with a relative speed unimaginably close the speed of light. Finally observe that after such a collision charged hadrons will fly at a large detector in a pattern where there is an average separation of charge. This separation of charge is called the Chiral Magnetic Effect (CME) and this effect is studied thoroughly by a large number of physicists.

CME is found to be caused by anomalous parity-symmetry violating effects, which happen during the collisions. However, extracting the CME from background effects, has proven to be challenging. By utilising the Anomalous Viscous Fluid Dynamics simulation framework, we are able to configure quantitatively this parity-symmetry violating effect and also, separately, configure background effects. Data received from this simulation can be compared to the data from the ALICE detector at the LHC. Now, one could quantitatively describe this anomalous effect.
As these particles collide in the ALICE detector, two regions of the ions will overlap. This region will become very hot and dense. It is now a different state of matter, called the Quark Gluon Plasma, which is understood to be the state of matter a fraction of a second after the big bang.

To find this a mathematical description, azimuthal correlations between different charged particles embodied by various corralators will be studied. These correlators $\gamma_{m,n}$ can be constructed by using different integers for m and n, as will be described in section 3. The $\gamma_{m,n}$ correlator is said to be the $|m+n|^{th}$ order correlator. Different order correlators will approximate different shapes of the overlap region of the QGP. As will be described in section 2, the parity-symmetry violating effects are configured by means of an initial state parameter n_5/s, which reflects the initial chirality imbalance in the system. The background effects we measure are found to be a direct result of Local Charge Conservation (LCC), which is a result of particle decay. This is a parameter which can be configured in the final state of the simulation. The effects of these parameters on the mentioned higher order correlators will

be essential to quantify the anamolous chirality imbalance, observed at the LHC.

2 Anomalous Viscous Fluid Dynamics Simulation

After finding the experimental results from the ALICE detector, we want to study exactly the degree to which this is a result of a chirality imbalance. A rather large portion of the measured signal is due to local charge conservation. As the experiment is being simulated with MonteCarlo integration, it is important that one can configure these effects into the simulation. The Anamolous Viscous Fluid Dynamics Framework [3][4][5] is able to provide this.

In a collision between nuclei at LHC energies, a region of the two nuclei will overlap. Because of the high colliding energy, this region will heat up immensely and will become very dense. This is considered to be a different state of matter called the quark gluon plasma. In this state, color charges can move separately, hence it is called a plasma. The moment of collision is used as the initial state of the AVFD simulation. Recent research on the quark gluon plasma has found that its equations of motion resemble that of a viscous fluid. Hence, this framework is used to simulate the expansion of the QGP.

2.1 Net-chirality and LCC

Experimental data described in section 3, conclude that a separation of charge is found. This can happen in part by a net-chirality. Looking at Fig. 1 on the left picture, one can see the alignments of positive particle's spin vector in the direction of the magnetic field. In turn, the left handed particles will move in a trajectory opposite to the magnetic field. The right handed particles will do so in the direction along the magnetic field. From this, no measurable current is observed, since the amount of charged particles is the same in both directions. In the middle picture a net-chirality is introduced. The parameter μ_5 quantifies the imbalance and is thus closely related to the chiral axial current within the AVFD framework. In practice the net-chirality implies that there are more left handed particles than right handed particles.

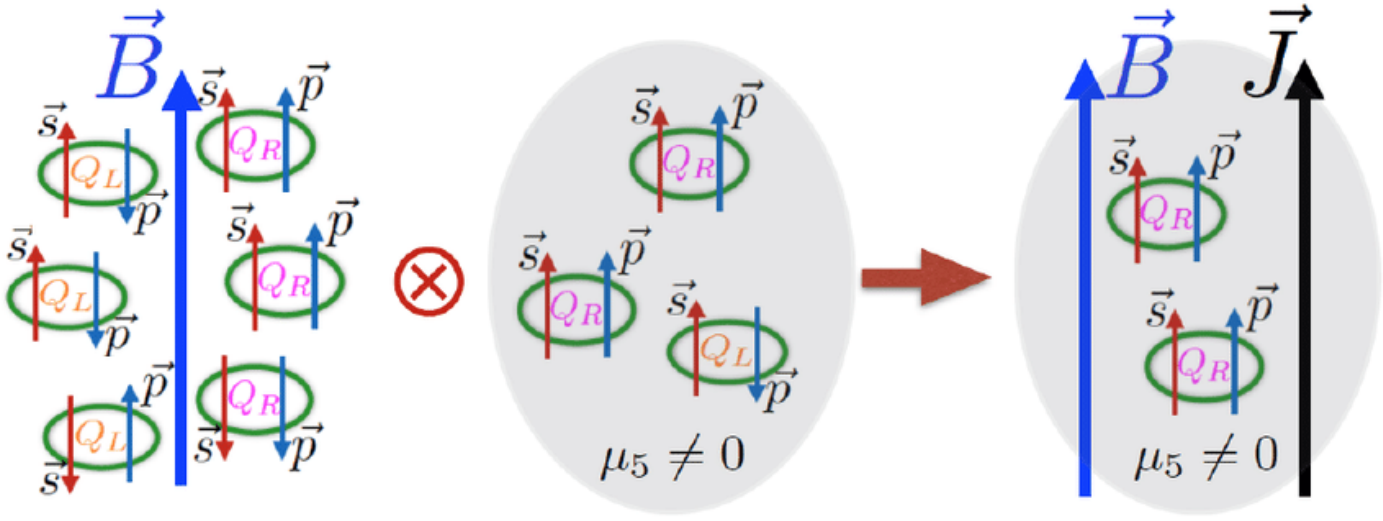

Figure 1: This figure shows a schematic explanation of a current as a results of a chirality imbalance and a magnetic field, for positive quarks [2]

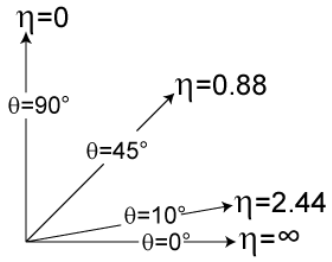

Figure 2: This figure shows an intuitive visualization of pseudorapidity η [7].

The right picture now shows a combination of the other two pictures. Since more right-handed particles are found, there are more positive particles moving along the B field than in opposite direction. Since the equivalent negative particles have an opposite spin polarization, we can conclude that the same current for negative particles is found in opposite direction.. This phenomenon can now be interpreted as a current. The value n_5/s is configured for a specific value in the initial state of the simulation.

As mentioned before, the net-chirality isn't the only cause for getting non-zero values for charge separation. After the collision, the quark gluon plasma will expand and therefore decrease in temperature. In this phase hadrons can form from these quarks. Now, these hadrons can decay. The decay products coming from these hadrons might have separate charges and, as one might expect, have an influence on the correlator values. This effect is called 'Local Charge Conservation' (LCC) and can be implemented in the final state of the simulation.

After the collision only the particles that are a direct result of the quark gluon plasma will be considered and therefore simulated. The particles scattering of from the region which isn't the overlap region, also called spectators, are neglected.

2.2 Analysis details

For each event, the simulated data will have used a specific value for the centrality parameter in the initial state. Centrality is closely related to the impact parameter b, which is defined as the distance between the centers of the lead ions during the collision, see Fig. 3. The values of the impact parameter considered in this paper will be between 0 and 20 fm. The centrality has a complex definition defined in [6] and will be considered in percentage ranges. As the impact parameter gets bigger so does the centrality. To do the calculations more easily, the values will be considered to be within an interval. The intervals considered are 0-10 10-20, 20-30, 30-40, 40-50, 50-60 60-70 % centrality.

In order to get a meaningful description of the effects of interest, The AVFD simulation can be constrained to specific ranges of pseudorapidity η to match the experimental acceptance of ALICE. Pseudorapidity is defined according to

$$\eta = -ln[tan(\frac{\theta}{2})] \tag{1}$$

where θ is the polar angle, defined as the angle between the beam-axis and the axis of the particle's velocity, see Fig.2.

With LCC and n_5/s configured for different values, we can observe their influence on the charge separation at the moment of measurement. As some higher order correlators might only give an indication of measured values due to background effects, it is possible to find the exact value of LCC when the experiment is performed. After this, one can produce results for $\gamma_{1,1}$ with this LCC value for multiple values of n_5/s . Preferably the curves will overlap for a specific value of n_5/s. Now a relation can be found between the centrality of the events and the anomalous chirality imbalance.

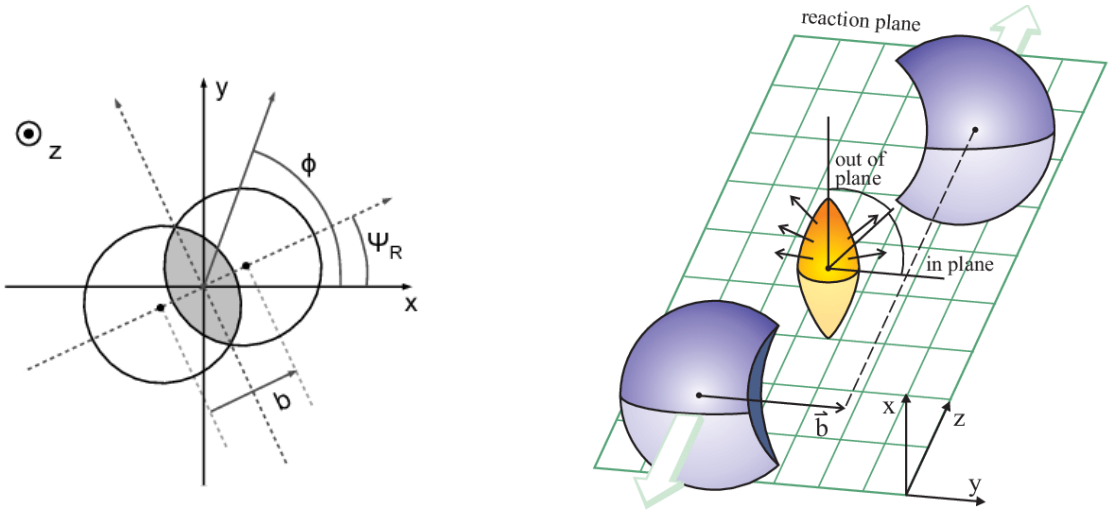

Figure 3: This figure shows 2 schematic representations of a collision, relating the impact parameter b and the angle of the reaction plane Ψ_{RP}. In the right picture, the magnetic field is directed in the positive x-direction. (Left figure from Ref. [8] and right figure from Ref. [9])

3 CME Correlators

In order to get a good quantification of the CME signal it is helpful to study azimuthal angle correlations between charged particles. [10] The correlators introduced in this section will be analyzed extensively.

3.1 The definition of the $\gamma_{m,n}$ correlators

The ALICE detector will measure the azimuthal angle ϕ_α of a particle α with respect to the lab as well as its electric charge . It will collect this data for multiple hadrons coming from the QGP for multiple collisions. The charge seperation due to the Chiral Magnetic Effect will be along the induced magnetic field. We can define a Reaction Plane as the plane that sits perpendicular to this magnetic field. It can be constructed from the beam axis and the axis of the impact parameter b, which is the axis laying in both centers of the colliding particles at the moment of collision, as shown by Fig. 3. The azimuthal angle of this plane Ψ_{RP} is now the angle of reference. The most famous among the correlators is $\gamma_{1,1}$, which describes, as the name implies, correlations between particles:

$$\begin{aligned}
\gamma_{1,1} &=< cos(\phi_\alpha + \phi_\beta - 2\Psi_{RP}) > \\
&=< cos(\phi_\alpha - \Psi_{RP} + \phi_\beta - \Psi_{RP}) > \\
&=< cos(\Delta\phi_\alpha + \Delta\phi_\beta) > \\
&=< cos(\Delta\phi_\alpha\Delta\phi_\beta) > - < sin(\Delta\phi_\alpha\Delta\phi_\beta) > \\
&=< v_{1,\alpha}v_{1,\beta} > + B_{in} - < a_{1,\alpha}a_{1,\beta} > - B_{out}
\end{aligned} \tag{2}$$

Where B_{in} and B_{out} represent the parity conserving correlations with respect to the in- and out-of-plane directions of the symmetry plane. The $< a_{1,\alpha}a_{1,\beta} >$ term describes the magnitude of the parity violating effects. For α and β we either choose particles which have the same sign electric charge (SS) or opposite sign (OS). This will now give a clear indication of how correlated particles with same sign and of how correlated particles with opposite sign are. The first and second term on the RHS describe the correlations with respect to the in- and out-of-plane directions respectively.

To generalize equation 2, we can define the $\gamma_{m,n}$ correlator:

$$\begin{aligned} \gamma_{m,n} &=< cos(m\phi_\alpha + n\phi_\beta - (m+n)\Psi_{|m+n|}) > \\ &=< cos(m\Delta\phi_\alpha + n\Delta\phi_\beta) > \end{aligned} \tag{3}$$

Also note that:

$$\begin{aligned} \gamma_{-m,-n} &=< cos(-m\phi_\alpha - n\phi_\beta + (m+n)\Psi_{|-m-n|}) > \\ &=< cos(-(m\phi_\alpha + n\phi_\beta - (m+n)\Psi_{|-(m+n)|})) > \\ &=< cos(m\phi_\alpha + n\phi_\beta - (m+n)\Psi_{|m+n|}) > \\ &= \gamma_{m,n} \end{aligned} \tag{4}$$

Entering into our equation m=1 and n=1, will give back equation 2 with $\Psi_{RP} = \Psi_2$. For more peripheral events the overlap region is well approximated by an ellipsoidal shape. The azimuthal angle of the short axis Ψ_2 of the ellipsoid, in the initial state, corresponds to Ψ_{RP}. The plane defined by the beam axis and the azimuthal angle Ψ_n is named the n^{th}-order symmetry plane.

For more central collisions, the initial state will not be properly described by an ellipsoid. On the other hand the overlap region for more central events will have a more disorganized shape. One way to study these events is to approximate the overlap region with different shapes. For instance when setting m=1 and n=2, we now have a mathematical description for finding correlations when the overlap region has a smooth triangular distribution. The symmetry plane of reference of this correlator will have angle Ψ_3. This angle is not correlated with that of the plane of reference and thus when a signal is found it will be a result of background effects by construct. This correlator is one of the two that will be studied. One other correlator which will be studied is $\gamma_{-1,3}$. Just like $\gamma_{1,1}$ and $\gamma_{1,2}$ this correlator can be associated with a specific shape of the overlap region. $\gamma_{-1,3}$ will give a mathematical description of correlations of particles for when the overlap region approximates a square. Just like $\gamma_{1,1}$ it will have Ψ_2 as its angle of reference. Now we have a different correlator which will be able to pickup CME-signals.

By filling values for m and n the following mathematical formulations can be found:

$$\gamma_{1,1} = < cos(\phi_\alpha + \phi_\beta - 2\Psi_2) > \tag{5a}$$
$$\gamma_{1,2} = < cos(\phi_\alpha + 2\phi_\beta - 3\Psi_3) > \tag{5b}$$
$$\gamma_{1,-3} = < cos(\phi_\alpha - 3\phi_\beta + 2\Psi_2) > \tag{5c}$$
$$\gamma_{2,2} = < cos(2\phi_\alpha + 2\phi_\beta - 4\Psi_4) > \tag{5d}$$
$$\tag{5e}$$

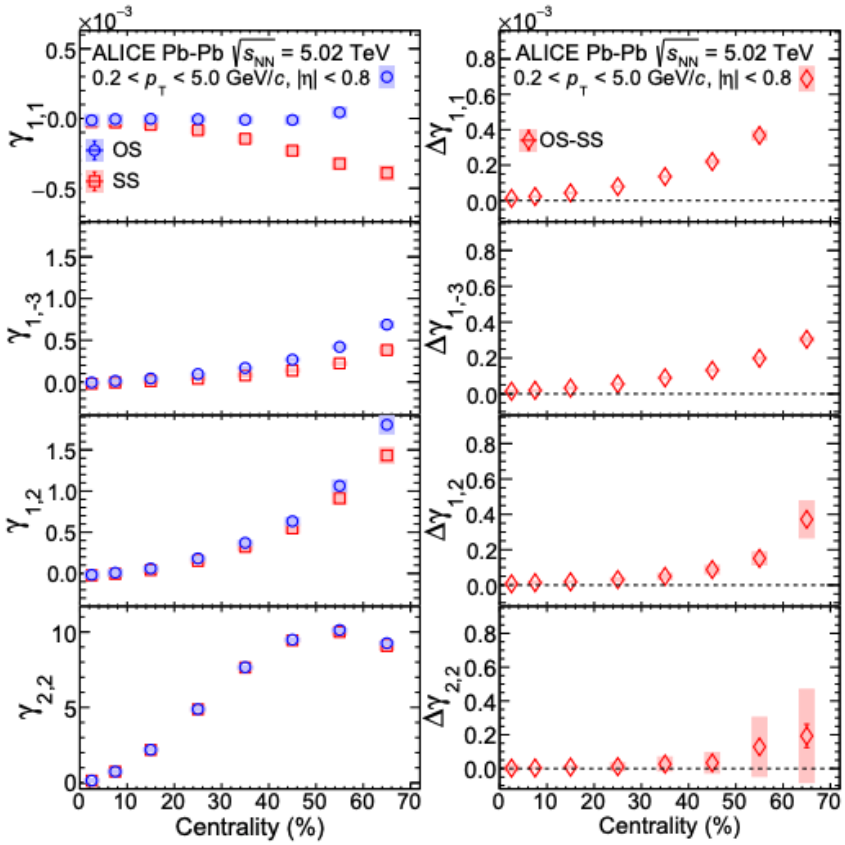

Figure 4: Experimental results plotted for multiple γ correlators. On the left panel separate values are shown for correlations between opposite sign and same sign. On the right panel the difference $\Delta\gamma$ correlators. [11]

3.2 The experimental results

After the data from the LHC is collected the particle correlations are calculated. The results [11] are shown in Fig. 4. The x-axis of both panels show the centralities. The y-axis on the left panel shows the found values for the corresponding γ. The blue markers represent the found values for the combinations of particles having opposite charges. The red markers represent the found values for the combinations of particles having the same electric charges. To take the latter as an example, the gamma correlator is calculated for all particle combinations where both particle α and β have the same charge. The y-axis on the right panel of Fig. 4 displays the difference in these values. I.e. $\Delta\gamma_{m,n} = \gamma^{OS}_{m,n} - \gamma^{SS}_{m,n}$.

It becomes apparent from Fig. 4 that for different γ correlators, different relations occur in the observed results. The $\gamma_{1,1}$ correlator shows a large difference in the combinations of OS and SS for an increased centrality. The values of γ for combinations of opposite sign particles increase and the values decrease with those of same sign. It becomes clear, by using this correlator, that one would indeed measure a signal. Now, looking at the $\gamma_{-1,3}$ correlator,

it becomes apparent that a slightly different pattern emerges. As the events become more peripheral, the $\gamma_{-1,3}$ is able to pick up a stronger signal. However, as plotted in the left panel, more peripheral events will have a positive value on the y-axis for both combinations of opposite sign electric charge and same sign electric charge. As a result, the difference will have a general smaller $\Delta\gamma$ value. Now, the same becomes visible for the $\gamma_{1,2}$ correlator. It shows even steeper curves on the left panel. However, again the difference between correlations of opposite charges and same charges is less defined, i.e. they have a similar curve.Since this correlator doesn't pick up any signal as a result of the chiral magnetic effect, it becomes a good indicator of background effects. The $\gamma_{2,2}$ correlator won't be discussed any further in this thesis.

4 Results

The results discussed in this section have been done so by considering calculations over the simulated data, which include both $\gamma_{1,2}$ and $\gamma_{-1,3}$. To understand the Chiral Magnetic Effect there will be separate simulation data for configured values of local charge conservation and n_5/s, over which the same calculations will be done. For each of these configurations 100k events will be simulated per centrality range. Only the primary particles, coming from the collision with an electric charge, will be considered, since none of the above configurations will have an effect of interest on neutrally charged particles. Furthermore, to match the experimental acceptance of the ALICE, the particles from the simulated data will be confined to the range $|\eta| < 0.8$ and $0.2 < P_T < 5.0 GeV/c$. Where the transverse momentum P_T is defined as the momentum in the radial direction.

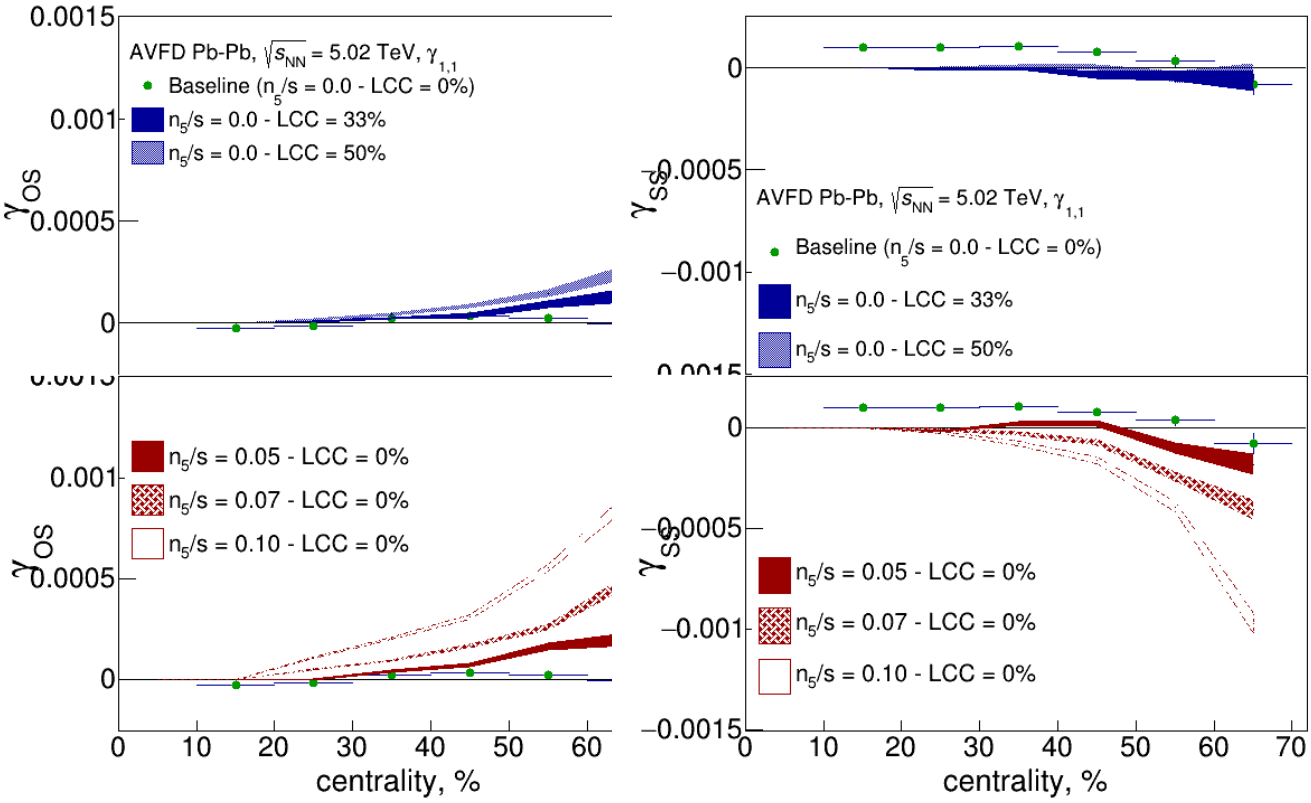

(a) $\gamma_{1,1}$ for particles with opposite sign electric charge.

(b) $\gamma_{1,1}$ for particles with same sign electric charge.

Figure 5: The $\gamma_{1,1}$ for particles with opposite sign electric charge and same sign electric charge are plotted with $n_5/s = 0; LCC > 0$ (above) and with $n_5/s > 0; LCC = 0$ (below).

4.1 The $\gamma_{1,1}$ correlator

Before considering these two correlators, describing the simulation result for $\gamma_{1,1}$ can be convenient as a reference. Fig. 5a shows the $\gamma_{1,1}$ correlator for combinations between particles having opposite charges. The x-axis shows the centrality of the collisions and the y-axis shows the value of the correlator. The figure is divided into 2 panels, with the upper panel presenting the value of $\gamma_{1,1}$ as a function of centrality for when n_5/s is fixed at 0 in the initial state of the AVFD simulations. The different graphs in this plot are for different configured values of LCC in the final state, which are directly related to background signals one might measure. The green markers represent the values for the same calculations when n_5/s and LCC are both configured to be 0 in the AVFD simulation which will be called baseline. The plot below will show the same correlator for when LCC=0 and multiple values of $n_{5/s}$. Fig. 5b shows the same for correlations of particles with the same electric charge.

The upper panel of Fig. 5a shows that the different values of Local Charge Conservation influence the $\gamma_{1,1}^{OS}$ correlator. The baseline fluctuates around 0. Above the baseline, it can be observed that an increased value of LCC will result in an increase of the γ value. The correlations of particles with same sign electric charge, seem to be less affected by local charge conservation, as indicated by the above panel of Fig. 5b. There also seems to be a decrease for these centralities. From analysing the lower two panels it becomes apparent that the configured values of n_5/s affect the output $\gamma_{1,1}$ a lot more.

Comparing these simulated data with the experimental results shown in the above panels of Fig. 4, a similar trend is visible for some possible combination of these configured parameters. As the centrality increases so do the values of γ_{OS} for positive values of LCC and

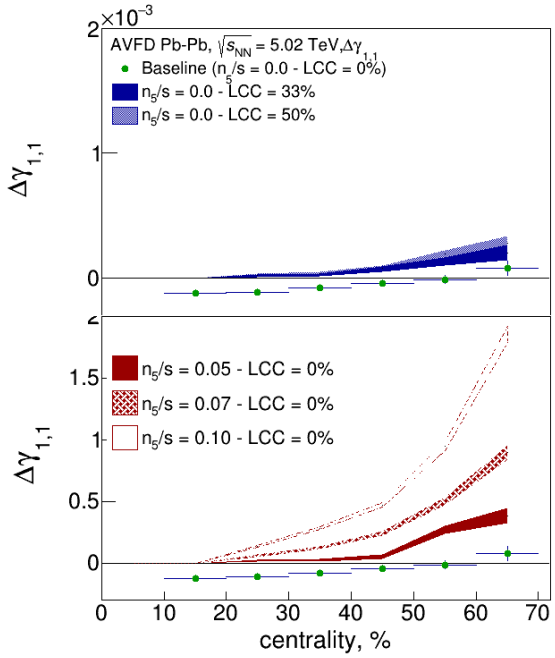

Figure 6: This figure shows the $\Delta\gamma_{1,1}$ correlator as a function of centrality, from the AVFD simulation data [12].

n_5/s, whereas the values decrease for γ_{SS} as these parameters are configured for the same values. Because the simulated values fluctuate around zero for when n_5/s and LCC are also zero, now it becomes visible that the experimental data suggest local charge conservation and net-chirality are most likely present in this system.

In Fig. 6 the difference between the $\gamma_{1,1}$ correlators for combinations of opposite sign and same sign electric charge are shown with respect to the centralities, i.e. $\Delta\gamma_{m,n} = \gamma^{OS}_{m,n} - \gamma^{SS}_{m,n}$. As is also visible from Fig. 5 the configured values of LCC increase the value of the $\Delta\gamma$ correlator and even more so do the configured values of n_5/s. This, in turn, means that the $\Delta\gamma$ correlator is indeed detecting a charge dependant current as a result of a chirality imbalance and also that local charge conservation present in the system will result in a similar measurement.

4.2 The $\gamma_{1,2}$ correlator

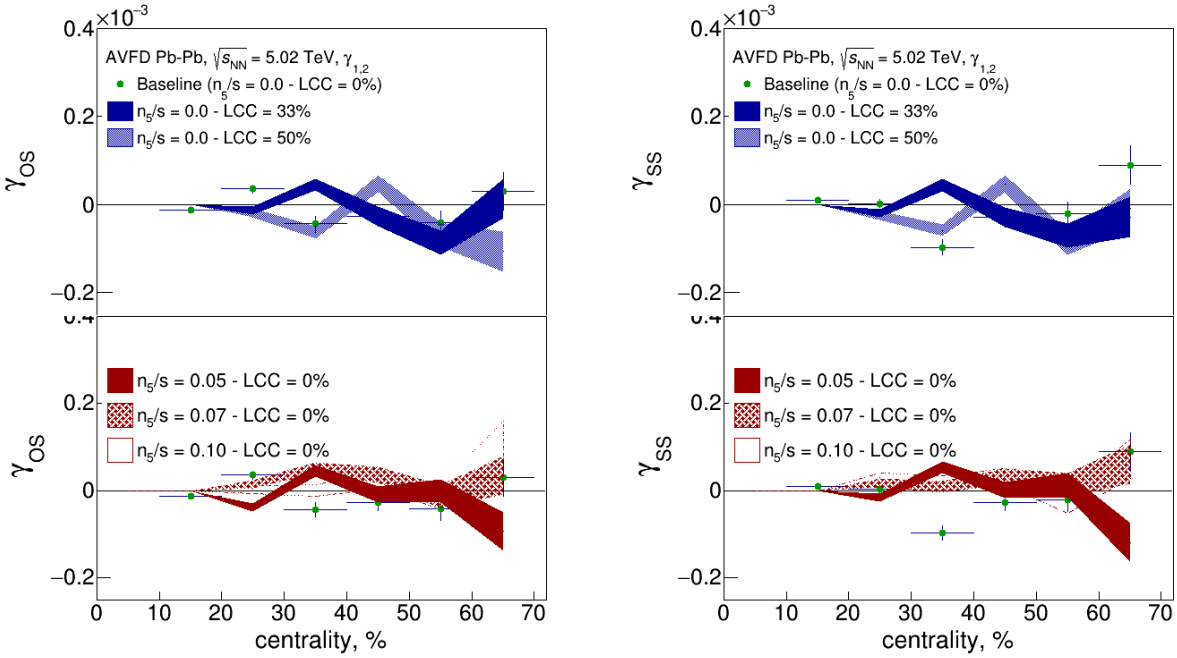

(a) $\gamma_{1,2}$ for particles with opposite sign electric charge.

(b) $\gamma_{1,2}$ for particles with same sign electric charge.

Figure 7: The $\gamma_{1,2}$ for particles with opposite sign electric charge are plotted with $n_5/s = 0; LCC > 0$ (above) and with $n_5/s > 0; LCC = 0$ (below).

Fig. 7a shows the relation of centrality and the $\gamma_{1,2}$ correlator much like it does for the $\gamma_{1,1}$ correlator in Fig. 5. The $\gamma_{1,2}$ correlator as mentioned in section 2 uses the the 3^{rd}-order symmetry plane as a plane of reference. This will therefore be a measure of any background signals. When comparing Fig. 7a and Fig. 7b it is apparent that the overall magnitude and shapes are very similar. The baseline points for opposite sign and same sign fluctuate around 0. The fact that it does not constantly increase/decrease with higher centrality indicates that

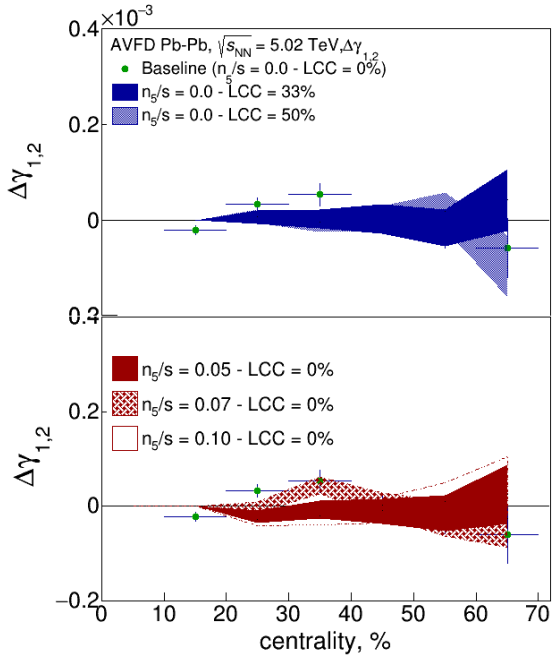

Figure 8: This figure shows the $\Delta\gamma_{1,2}$ correlator as a function of centrality, from the AVFD simulation data [12].

this is due to normal statistical fluctuations. This is also a clear reason why the Baseline values aren't the same for opposite sign and same sign. Now when we start looking for the measured values of γ_{os} and γ_{ss} for when there is a configured LCC at the final state, we can see that there are deviations in the same pattern, however with increasing values of Centrality, there isn't a well defined correlation to be observed. When increasing values of LCC the values also don't seem to be more defined than with smaller values. This all hints at an observation of deviation due to statistical fluctuations and therefor, no observed γ_{12} correlations with implemented Local Charge Conservation. Now looking at the bottom 2 panels, the same can be said for when there is a configured net chirality (n_5/s). Also, one can observe fluctuations around $\gamma = 0$ for different centralities. No clear pattern arises with increasing values of implemented net-chirality. The observation of the small difference is visible in Fig. 8. The $\Delta\gamma_{1,2}$ difference correlator shows no significant values. Neither the above nor the below panel show an influence of LCC or n_5/s. This correlator could give us an indication of any charge dependant background effects, but no such effects are found.

When looking at Fig. 9, again on the y-axis the values of $\gamma_{1,2}$ are plotted, but for a specific centrality range, picked at 50-60%. Now, the top and bottom graphs represent the values for γ correlations with opposite and same sign, respectively. Fig. 9a and 9b show on the x-axis the different values of the configured net-chirality and local charge conservation respectively. Just like Fig. 8 it is visible from these 4 plots, that no significant correlation is found.

As for the configured non-zero values of n_5/s, this can be explained by the fact that the mathematical description of $\gamma_{1,2}$ uses a plane of reference which does not approximate that of the reaction plane, i.e. it looks for a current, which is not in fact, in the direction of the magnetic field. The CME signal induced by implementing net-chirality will therefore not be

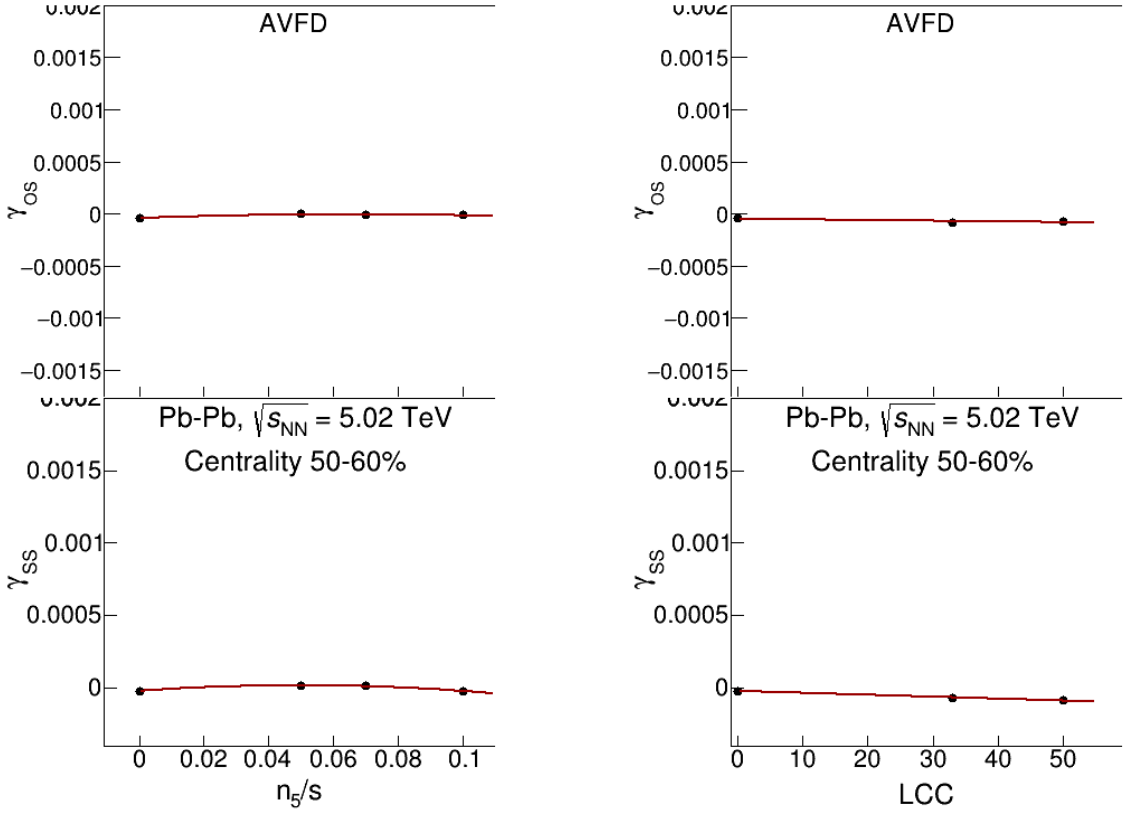

(a) $\gamma_{1,2}$ correlator as a function of n_5/s for particles with the same sign and opposite sign electric charge.

(b) $\gamma_{1,2}$ correlator as a function of LCC for particles with the same sign and opposite sign electric charge.

Figure 9: The $\gamma_{1,2}$ correlator as a function of different configured parameters which contribute to a current in the detector

in this direction and will not be measured by this correlator.

When describing background effects, however, these should be as a result of implemented non-zero LCC values. However, no such effects are measured. This isn't necessarily a trivial result. It has some different possible causes. For instance, it could mean that there is no cause for a non-CME signal in the direction perpendicular to Ψ_3, or that the overlap region can not be approximated well by a triangle.

4.3 The $\gamma_{-1,3}$ correlator

Fig. 10 describes in the same manner as Fig. 5 the calculated values for $\gamma_{-1,3}$ as a function of different centralities. First of all, the baseline values seem to be quite different for opposite sign and same sign. For, when the $\gamma_{-1,3}$ correlator is found for particles with opposite sign, the baseline increases with increasing centrality. This is also the case for particle correlations with the same sign. However, the former correlator seems to be more affected by centrality.

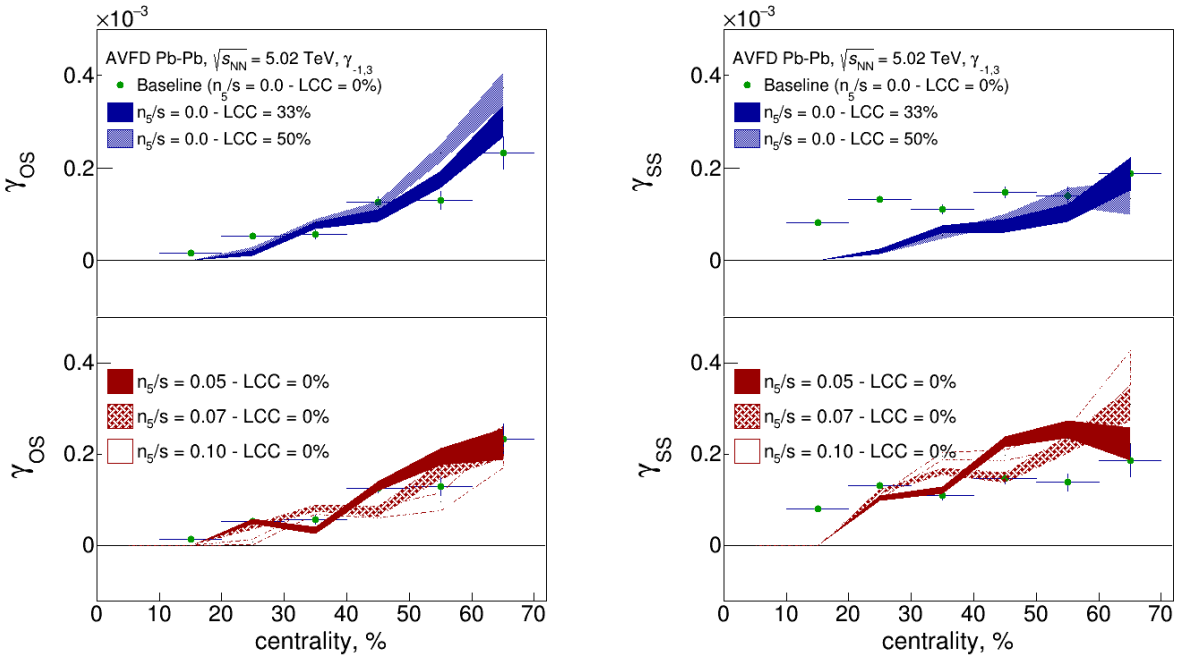

(a) $\gamma_{-1,3}$ for particles with opposite sign electric charge.

(b) $\gamma_{-1,3}$ for particles with same sign electric charge.

Figure 10: The $\gamma_{-1,3}$ for particles with opposite sign electric charge are plotted with $n_{5/s} = 0; LCC > 0$ (above) and with $n_{5/s} > 0; LCC = 0$ (below).

For when the centralities are in a range of 10-20%, the value of γ is closer to 0, and increases more with increasing centralities.

Now, looking at configured values of n_5/s, we can see that all three values will fluctuate around those of baseline. Again, meaning that no significant CME signal is found when implementing net-chirality. Only when looking at the very last centrality range of 60-70% of Fig. 10b that there is a correlation between γ_{SS} and n_5/s. However, for this range the simulation data is less reliable. It should also be noted that the value of γ_{SS} increases with increasing n_5/s. This is not what would be expected with a configured net-chirality.

Now, looking at the above plot of Fig. 10a, we can see a pattern, where an increase in local charge conservation is implemented, a slight increase of background signals is observed. This is also evident by the above plot in Fig. 12b. In this plot it seems that there is a slight increase in $\gamma_{-1,3}$ for higher values of implemented LCC. For γ_{SS}, however, this is not the case.

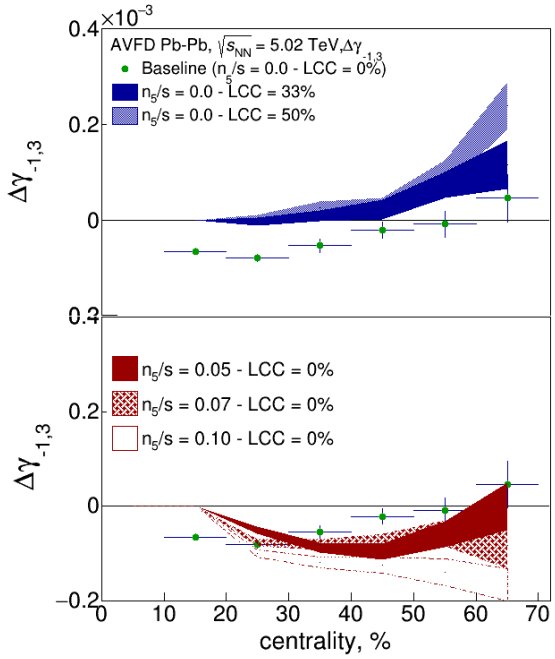

Figure 11: This figure shows the $\Delta\gamma_{-1,3}$ correlator as a function of centrality, from the AVFD simulation data [12].

Fig. 11 shows the $\Delta\gamma_{-1,3}$ difference correlator. From this correlator one can visualize the trend described for Fig. 10. The value of γ will increase for when the LCC is configured for higher values. Looking at the panel below, there might be a correlation visible for the difference in particle correlations for when there is a implemented value for n_5/s, but it would be small.

So what does this mean exactly? Looking at Fig. 7 it is apparent that using the $\gamma_{1,2}$ correlator to distinguish a CME-signal from background effects will not be effective with these simulated data. No significant correlations are found.

Now, when looking at Fig. 10 there is no clear measured CME-signal. It might give us a small indication of how local charge conservation is related to the centrality of the events. Suppose, there is a measured current found at the ALICE detector. If one now wants to understand how chirality is related to the centrality of Pb-Pb collisions, one first must find what part of the measured signal is due to background effects. Since this $\gamma_{-1,3}$ correlator potentialy only shows a significant structure for when LCC is found. We can now calculate exactly the value of LCC and then use the $\gamma_{1,1}$ correlator, now one can subtract the part of the measured signal due to local charge conservation, to find what n_5/s is for different centralities.

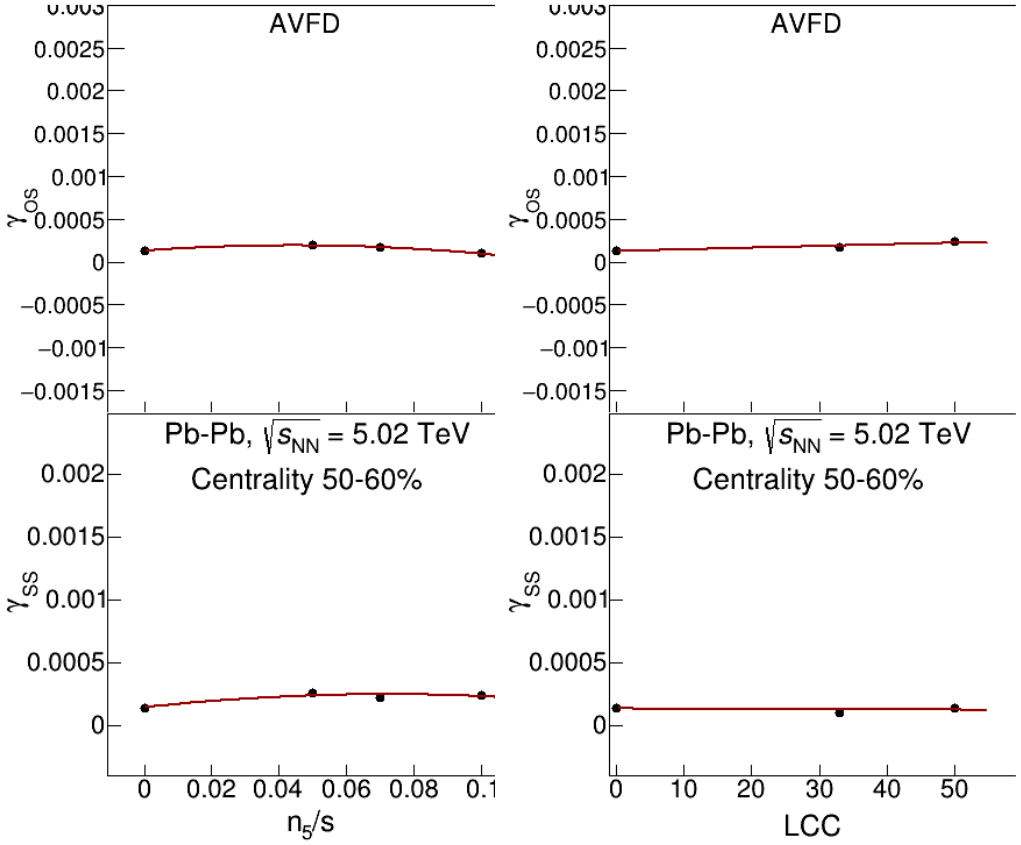

(a) $\gamma_{-1,3}$ correlator as a function of n_5/s for particles with the same sign and opposite sign electric charge.

(b) $\gamma_{-1,3}$ correlator as a function of LCC for particles with the same sign and opposite sign electric charge.

Figure 12: The $\gamma_{-1,3}$ correlator as a function of different configured parameters which contribute to a current in the detector

5 Outlook

5.1 The $\Delta\gamma_{1,2}$ correlator

Now it is important to compare the simulated data with the experimental data. As we can see from Fig. 13b for a 60-70 % centrality range the measurement is a value of $\Delta\gamma_{1,2}$ of about $0.35 * 10^{-3}$. For the implemented values of n_5/s and LCC, the value of $\Delta\gamma_{1,2}$ gets no higher than $-0.1 * 10^{-3}$. as discussed previously, for n_5/s this is to be expected, however it is possible that Local Charge Conservation does have an effect on the correlator value.

Looking at all the configured values of LCC and n_5/s from 13a, it is visible that there is a lot of fluctuation present in this system. The Baseline markers fluctuate just as much as for different configurations. This means that from this figure no significant information is found on the effects of n_5/s and LCC on the $\gamma_{1,2}$ correlator. As the uncertainty is relatively big to the measured values of the experimental results, an AVFD simulation must be done with more events. This will reduce the observed fluctuations and one can potentially obtain significant information of the effects.

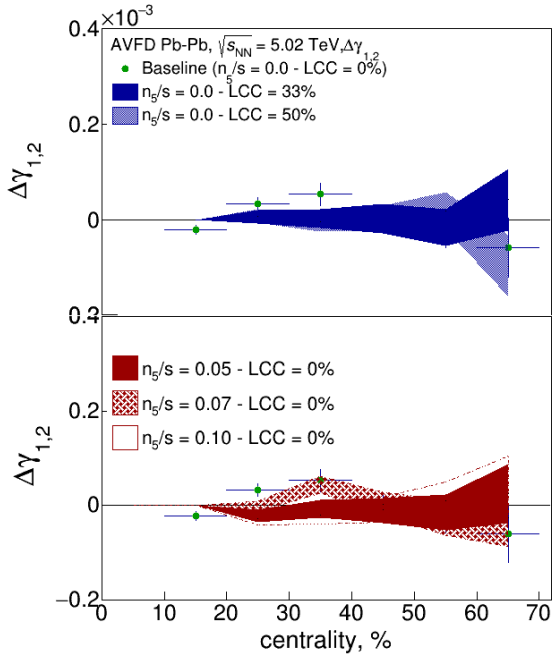

(a) $\Delta\gamma_{1,2}$ correlator as a function of centrality for simulated data.

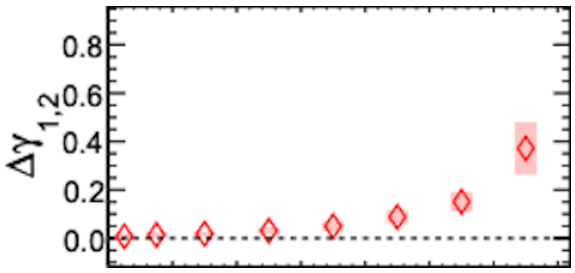

(b) $\Delta\gamma_{1,2}$ correlator as a function of centrality for experimental findings.

Figure 13: Comparison between the simulated data and experimental data for $\Delta\gamma_{1,2}$ correlator. The y-axis shows the value of the $\Delta\gamma_{1,2} * 10^3$

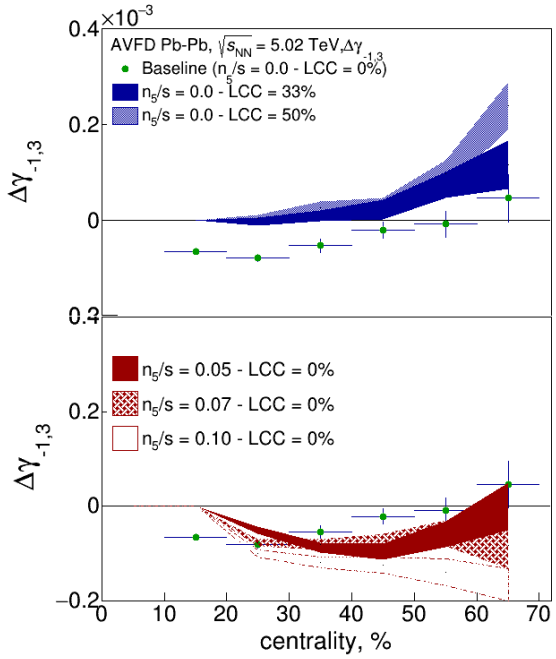

(a) $\Delta\gamma_{-1,3}$ correlator as a function of centrality for simulated data.

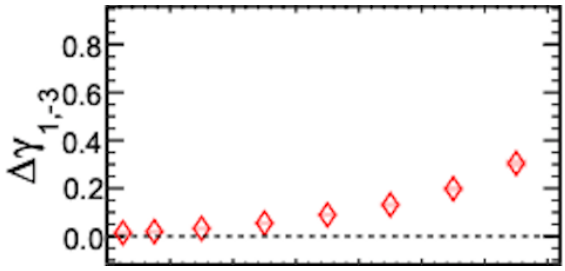

(b) $\Delta\gamma_{-1,3}$ correlator as a function of centrality for experimental findings. The y-axis shows the value of the $\Delta\gamma_{-1,3} * 10^3$

Figure 14: Comparison between the simulated data and experimental data for $\Delta\gamma_{-1,3}$ correlator. The y-axis shows the value of the $\Delta\gamma_{-1,3} * 10^3$ for the right panel

5.2 The $\Delta\gamma_{-1,3}$ correlator

When looking at Fig. 14, there is a bit more significant information to be extracted. In Fig. 14b the value of $\Delta\gamma_{-1,3}$ is about $0.35{*}10^{-3}$. When comparing this to Fig. 14a it is visible that for $LCC = 50\%$, this value is about $0.3{*}10^{-3}$. As mentioned before, the n_5/s parameter does not show a significant relation with the $\Delta\gamma_{-1,3}$ correlator, when configured in the simulation. To study this relation further, it is again important to reduce the fluctuations. This means that more simulations need to be done. It could as well be the case that the $\Delta\gamma_{-1,3}$ correlator gets reduced by increasing the n_5/s parameter. If this is the case, more and higher values of LCC should be configured in the simulation in order to approximate the right panel.

When looking at Fig. 15 we have found value ranges of the two parameters to fit $\Delta\gamma_{1,1}$, as described in [12]. Now looking back at 14b, it is now possible to do a prediction. If one were to do the same simulation for more events, plugging in $LCC \sim 60\%$ and $n_5/s \sim 0.03$, might make the experimental results overlap. These values are within the ranges displayed in Fig. 15 and so the $\Delta\gamma_{-1,3}$ correlator might help us understand the experimental findings better.

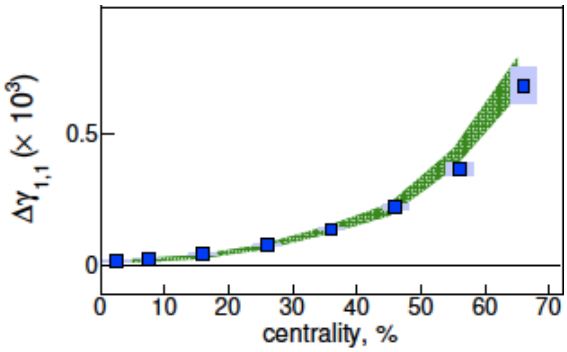

Figure 15: The blue markers show the experimental results for $\Delta\gamma_{1,1}$ done by ALICE and the green range show findings for $LCC = 40 - 60\%$ and $n_5/s = 0.02 - 0.05$ [12]

.

5.3 Final thoughts

As mentioned previously, these higher order correlators are a lot less sensitive to the Local Charge Conservation and net-chirality configurations, compared to the first order correlator $\gamma_{1,1}$. This means that, in order to make these higher order correlators contribute to finding these parameters from the experiments, more events need to be simulated. As becomes more and more clear, the statistical fluctuations influence the results too much. Also, when looking at the $\gamma_{-1,3}$ correlator it might be convenient to simulate for higher values of LCC. This might help getting closer to understanding the influence of Local Charge Conservation and net-chirality on the lead-lead collisions.

References

[1] J. Thaeder, T. Kolleger, and T. Alt (2012), general Photo, URL https://cds.cern.ch/record/1477949.

[2] D. Kharzeev, J. Liao, S. Voloshin, and G. Wang (2015).

[3] S. Shi, Y. Jiang, E. Lilleskov, and J. Liao, Annals of Physics **394**, 50–72 (2018), ISSN 0003-4916, URL http://dx.doi.org/10.1016/j.aop.2018.04.026.

[4] S. Shi, H. Zhang, D. Hou, and J. Liao, Physical Review Letters **125** (2020), ISSN 1079-7114, URL http://dx.doi.org/10.1103/PhysRevLett.125.242301.

[5] Y. Jiang, S. Shi, Y. Yin, and J. Liao, Chinese Physics C **42**, 011001 (2018), ISSN 1674-1137, URL http://dx.doi.org/10.1088/1674-1137/42/1/011001.

[6] B. Abelev, J. Adam, D. Adamová, A. M. Adare, M. M. Aggarwal, G. Aglieri Rinella, M. Agnello, A. G. Agocs, A. Agostinelli, Z. Ahammed, et al., Physical Review C **88** (2013), ISSN 1089-490X, URL http://dx.doi.org/10.1103/PhysRevC.88.044909.

[7] Wikipedia contributors, *Pseudorapidity — Wikipedia, the free encyclopedia* (2021), [Online; accessed 12-June-2021], URL https://en.wikipedia.org/w/index.php?title=Pseudorapidity&oldid=1018871377.

[8] S. Chatrchyan et al. (CMS Collaboration), Phys. Rev. C **87**, 014902 (2013), URL https://link.aps.org/doi/10.1103/PhysRevC.87.014902.

[9] B. Betz, *Jet propagation and mach-cone formation in (3+1)-dimensional ideal hydrodynamics* (2009).

[10] S. A. Voloshin, Phys. Rev. C **70**, 057901 (2004), URL https://link.aps.org/doi/10.1103/PhysRevC.70.057901.

[11] S. Acharya, D. Adamová, A. Adler, J. Adolfsson, M. M. Aggarwal, G. Aglieri Rinella, M. Agnello, N. Agrawal, Z. Ahammed, and et al., Journal of High Energy Physics **2020** (2020), ISSN 1029-8479, URL http://dx.doi.org/10.1007/JHEP09(2020)160.

[12] P. Christakoglou, S. Qiu, and J. Staa, *Systematic study of the chiral magnetic effect with the avfd model at lhc energies* (2021), 2106.03537.